A Cascaded Feature Extraction for Diagnosis of Ovarian Cancer in CT Images

Arathi B[1]*, Shanthini A[2]
Research Scholar, Department of Data Science and Business Systems[1]
Associate Professor, Department of Data Science and Business Systems[2]
SRM Institute of Science and Technology, Kattankulathur, Tamil Nadu 603203[1, 2]

***Abstract*—This paper proposed ovarian cancer detection in the ovarian image using joint feature extraction and an efficient Net model. The noise of the input image is filtered by using Improved NLM (Improved Non-Local Means) filtering. The deep features are extracted using Deep CNN_RSO (Deep Convolutional Neural Network Rat Swarm Optimization), and the low-level texture features are extracted using ILBP (Interpolated Local Binary Pattern or Interpolated LBP). To improve the feature extraction and reduce the error, use a cascading technique for the feature extraction. RSO also helps to efficiently optimize the DCNN features from the images. Finally, the extracted image is classified using the Efficient Net classifier, which performs a global average summary and classification of ovarian cancer (normal and abnormal). The system's performance is implemented on the Cancer Genome Atlas Ovarian Cancer (TCGA-OV) dataset. The system's performance, like sensitivity, specificity, accuracy and error rates, shows better with respect to other techniques.**

Keywords*—Ovarian cancer; deep convolutional neural network rat swarm optimization; CT image; joint feature; efficient net; improved non-local means; interpolated local binary pattern

I. Introduction

Ovarian cancer (OC) a disease that affects women's ovaries, is difficult to diagnose early, and has a high fatality rate [1]. OC has the highest mortality rate and is the leading cause of gynaecological deaths. There are two primary forms of invasive ovarian cancer, often referred to as Type-I and Type-II tumours [2]. Low-grade endometrial carcinomas, Low-grade serous carcinomas, clear-cell carcinomas, mucinous carcinomas, and malignant Brenner (transitional) tumours are examples of early-stage, nonaggressive type-I malignancies [3] [4]. Seventy-five percent of epithelial ovarian malignancies are type II tumours, which include high-grade serous carcinomas, high-grade endometriosis carcinomas, undifferentiated carcinomas, and malignant mixed mesodermal tumours. CT scans are routinely used to diagnose ovarian tumours, detect metastases, determine the stage of ovarian cancer, monitor patients following surgery, and evaluate the success of treatment [5].

Some ovarian epithelial tumours do not seem to be malignant when examined in the lab, and they are referred to as borderline epithelial ovarian cancer. Screening tests and exams identify diseases in people with no symptoms, such as cancer [6]. The abdomen and pelvis CT scan is the first-line imaging modality for ovarian cancer staging, therapy options selection and disease response assessment. The imaging surrogate for surgical-pathological FIGO staging is the staging CT, which gives disease distribution and load. This is mostly due to late detection, although OC often recurs after treatment. The remarkable difference in cure between patients with close illness and those with distant disease (15% vs. 25%) eloquently illustrates the need for a non-invasive but feasible diagnostic applicable to a large population expected to be afflicted by OC in its early stages [7].

Regardless of the fact that OC is only the 6th most frequent female cancer in Singapore, it is still a leading cause of gynaecological cancer mortality. As a result, the risk of cancer increases throughout life [8], leading to some complications, such as the inability of women with OC to have children and a problem after menopause. Therefore, to overcome these problems for women, accurate identification, solid cancer analyses [9], and the treatment procedure need all be improved. Despite all of these efforts, early detection of OC continues as a critical concern [10, 11]. With the use of proteomic analysis in serum, there has been continuing study to detect new cancer indicators. The cause or causative factor for OC is unknown, making early detection of ovarian cancer difficult [12].

The link between OC diagnosis and survival led to thinking and efforts to improve the outcomes obtained at the early recognition phases. This information is used to make better informed decisions while saving money [13, 14]. There are five reasons why a big data strategy can help cancer detection. Pathologists also noticed and examined the numerous gene articulations in this specific OC as well as the amounts of gene articulating in distinct neurotic phases and situations [15], as part of the same inquiry. Both organic and statistical computing may be used to characterize gene articulations for such relationships [16], especially in dynamic conditions when the tumour progresses from the quantitative processing of OC tissue [17, 18]. Different X-ray absorption coefficients in the human body indicate tissue properties in CT scans. CT provides the advantages of quick scan time and accurate localization [19].

The number of lesions and the simplicity with which they may be imaged are more important than the expense of the imaging technique. Radiation is a type of energy that may injure the human body. The resolution of CT scans is very important [20]. According to the statistics and machine learning part, various classification approaches were utilized in the cancer classification process, although it has certain non-trivial job problems. The knowledge about gene

*Corresponding Author.

articulation is unlike anything else that these approaches have ever dealt with. The supervised learning method uses the training set of categorized data to create a classifier that can be used to classify new data.

1) Motivation: The recognition of CT images is difficult to identify using segmentation or clustering. It may have a greater impact on the FAR and FRR rate at the moment of identification from the knowledge base. Existing systems have a functioning accuracy level of 90 to 95. It may be improved so that the system classifies more precisely and efficiently. Previous techniques were unable to classify the cancer stage. The assessment of the patient's stage aids in the more efficient treatment of the patient. The presented issues of the system motivated to development of a new methodology known as joint feature extraction with an efficient net classifier for ovarian cancer detection.

2) Contribution

- To improve the feature extraction of the CT image, Joint feature extraction is introduced based on the fusion of high-level (deep) and low-level (shallow) features are introduced for performing better image feature extraction.
- The deep features are extracted using Deep CNN_RSO, and the low-level texture features are extracted using ILBP. Both techniques are used to reduce the error rate in feature extraction.
- The efficient Net classifier is used to categorize the ovarian CT image by minimizing the greatest number of features in the data without sacrificing its original properties and decreasing the processing time and memory space.

The structure of the paper: Section II gives the related works of ovarian cancer detection in the CT images, the proposed methodology describes in Section III, Section IV explains about the result and discussion, and Section V concludes the paper.

II. Related Work

Lu et al. [21] presented a technology based on learned and created a non-invasive reduction in the quantity of the main ovarian tumour. Despite best efforts, the five-year survival rate for epithelial ovarian cancer (EOC) is around 35–40 per cent, underlining the use of classification markers for tailored treatment. Here, extracted 657 quantifiable statistical characteristics from the data in this section. 364 EOC patients' pre-operative CT scans at their initial presentation. The "Radiomic Prognostic Vector" is made up of four descriptions (RPV). RPV has a high level of accuracy when it comes to identifying people. The 5% of people with a median survival rate of fewer than two years improves dramatically. Based on well-established prognostic methodologies and has been tested in two separate multi-centre cohorts. In addition, two separate datasets were analyzed genetically, proteomic and transcriptomic. The activation of the stromal phenotype and DNA damage response mechanisms are included.

Lago et al. [22] proposed the Sentinel lymph node technique for the early detection of ovarian cancer (SENTOV). Ovarian cancer in an early stage may be the optimal disease setting for lymph node monitoring. Nonetheless, it appears that the documented experience is limited. The purpose of this study was to evaluate the feasibility and safety of sentinel lymph node biopsy in patients with clinical stages I and II ovarian cancer. Twenty patients in total are being monitored. Sentinel lymph nodes were seen in 14/15 individuals. (93%) pelvic region and each of the twenty para-aortic regions (100%). Due to this, five individuals did not receive an utero-ovarian injection when the average time between injection and beginning of symptoms was reached. The resection of sentinel lymph nodes required 53–15 minutes (range; the average number of sentinel lymphocytes recovered was 30–80). There were 2, 21.50 lymph nodes in the pelvic region (range: 0–5).

Wang et al. [23] suggested non-invasive recurrence forecasting models in HGSOC that aggregate prognostic characteristics from pre-operative computed tomography (CT) images utilising a unique deep learning (DL) technique. Equipment and procedures include 245 HGSOC patients from two hospitals, including a feature-learning cohort (n = 102) and two independent validation cohorts (n = 49 and n = 45). To capture the prognostic biomarkers (DL feature) of HGSOC, 8917 CT images from the feature learning cohort were used to train a unique DL network. A DL-CPH model including the DL feature and Cox proportional hazard (Cox-PH) analysis was created to predict patient recurrence risk and three-year recurrence probabilities.

Castellani et al. [24] developed a standard pre-surgical staging for the identification of ovarian cancer. The most important prognostic factor in ovarian cancer is the stage of the disease at the time of diagnosis. The current staging system (FIGO classification) is based on clinical and histological results. Despite the fact that the clinical stage is the standard method in ovarian cancer, the first patient care relies on an imaging-based which was before staging evaluation to detect disease that is unrespectable or difficult to resect. Radiologists must know the advantages and disadvantages of the many imaging techniques available. For effective staging and treatment planning, a clear understanding of the path of disease dissemination and review regions is essential. CT scans of the chest, abdomen, and pelvis are the current standard of care for pre-surgical staging. This enables a quick assessment of the disease's severity and is cost-effective.

Funston et al. [25] described CA125, an excellent screening test for ovarian cancer in primary care, particularly for women under the age of 50. To avoid diagnostic delays, patients with increased CA125 values should be evaluated for non-ovarian malignancies, especially if ovarian cancer has been ruled out. Our findings allow physicians and patients to predict the risk of ovarian cancer and other malignancies at any CA125 level and age, which can be used to guide individual decisions about the need for additional testing or referral.

Nougaret et al. [26] proposed radio genomics and radionics computational ways to measure tumour heterogeneity to investigate the entire tumour heterogeneity rather than a single biopsy sample. Cancer heterogeneity has been identified at the genetic and histological stages of ovarian cancer and has been linked to poor health outcomes. In advanced ovarian cancer with peritoneal carcinomatosis, traditional magnetic resonance or computed tomography imaging methods do not allow for intra- or inter-tumor heterogeneity. Feature extraction, which involves extracting various variables from pictures and is an element of radionics', has subsequently been suggested to assess progressed ovarian tumour heterogeneity. This brief overview covers the fundamentals of radionics, how to do texture analysis, and how to apply it to ovarian cancer imaging.

Forstner et al. [27] propose a Standardization of imaging techniques for ovarian cancer detection. Early detection is the only way to achieve a high cure rate in females with ovarian cancer. Despite rapidly evolving biomarkers, there is still no viable technique for early detection. Ovarian cancer has a low prevalence, a low specificity, and a high sensitivity. False positive percentages have been one of the screening programmes' drawbacks. Transvaginal sonography and magnetic resonance imaging (MRI) are useful methods for identifying ovarian masses in the hands of professionals. Efforts to standardize procedure and analysis are now underway and are expected to continue. Improve clinical diagnostic capabilities and the usage of cancer risk prediction algorithms. Radiogenomics and Radiomics could provide a plethora of extra information in the diagnosis and treatment of ovarian cancer.

These studies about ovarian cancer detection in CT images show that many issues exist in the detection of ovarian cancer in the CT image, such as increased noise in feature extraction, classification error, low specificity and low sensitivity. To improve the method's performance and reduce the error, here propose a new methodology named ovarian cancer detection in CT image by joint feature extraction and Efficient Net classifier.

III. Proposed Methodology

Ovarian cancer is a type of cancer that affects the ovaries. The cells can enter and harm healthy biological tissue and grow rapidly. Most techniques failed to identify cancer in the CT image due to the error and noise in the output image. Here, the proposed ovarian cancer detection by joint feature extraction and efficient net classifier. In this case, the pre-processing technique is initially done by using Improved NLM filtering to remove unwanted noise in the image. Next, Joint feature extraction is done based on the fusion of high-level and low-level features. Here, the deep features are extracted using Deep CNN_RSO and the low-level texture features are extracted using ILBP. Both the features are cascaded to obtain joint feature extraction for performing ovarian image classification. Finally, the Efficient Net classifier performs a global average pooling and classification of normal and abnormal images. Thus, the suggested Efficient Net classifier can lower the maximum number of data features without altering their original properties and cut processing time and memory space. The performance of the presented approach will be examined with recent existing approaches in terms of performance metrics to prove the performance efficiency. The architecture of the proposed method is shown in Fig. 1.

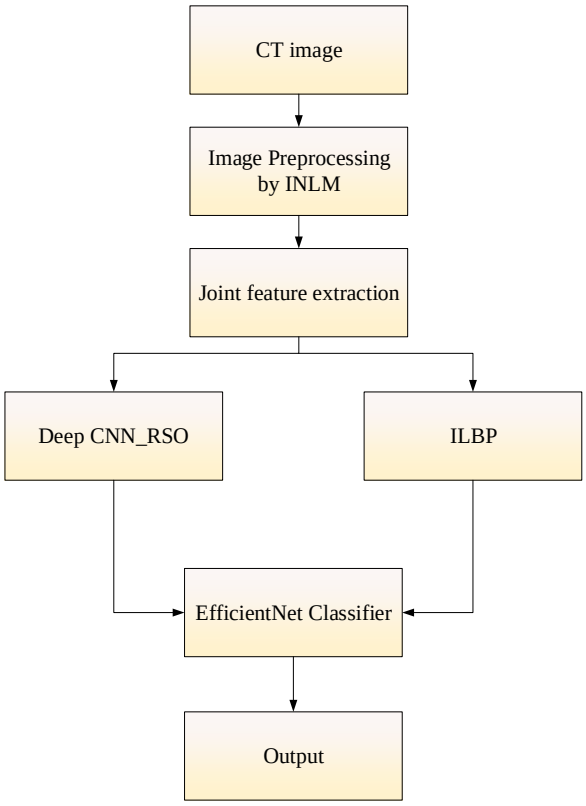

Fig. 1. Architecture of the proposed system.

A. Pre-processing

Image pre-processing is the preparation of images prior to their use in model training and inference. This covers orienting, resizing, and colour adjustments of the CT image. After collecting the CT images of ovarian cancer, upload the dataset picture and transform the RGB image into a grayscale image. Here pre-processing is done by using Improved Non-Local Means (INLM). According to the NLM, the weights are produced under the Gaussian noise assumptions that are used to quantify the closeness between a core area patch in a searching window and nearby patches. Only pixel data is used to construct the weights for the NLM, which quantifies the closeness between a centre area patch and its nearby patches. The variance is used to calculate the neighbourhood similarity measure. This similarity metric does not completely consider the structural data of the picture whenever the noise levels are too high in the case of NLM. There are errors generated in the case of noise in the CT images, so an improved NLM is used for the smooth region to achieve a better effect in the image, to provide good protection for the edge and the adaptive selection of the Gaussian weighting coefficients. The algorithm for INLM is shown below.

$$S = \frac{1}{\sqrt{3}P}\sum_{p=0}^{p=1}\left\| f_k(x,y) - g_k \right\|_2 \quad f_k(x,y) \in Patchwindow \qquad (1)$$

$$w(u,v)=\exp\left(-\frac{\sum_{p\in P}\left\| f_k(x+p,y+p)-f_k(x_0+p,y_0+p)\right\|_2^2}{h^2}\right) \quad (2)$$

$$w(x,y,x_0,y_0)=\exp\left(-\frac{\sum_{p\in P}\left\| f_k(x+p,y+p)-f_k(x_0+p,y_0+p)\right\|_2^2}{h}\right) \quad (3)$$

$$w_1(x,y,x_0,y_0)w_{21}(x,y,x_0,y_0)$$

$$g_k(x,y)=\frac{\sum_{u,v\in N} f_k(x+u,y+v)w(u,v)}{\sum_{u,v\in N} w(u,v)} \quad (4)$$

S Shows the general expression for the INLM algorithm, w represents the weight of the CT image and $g_k(x,y)$ shows the grey level representation of the image. The detailed algorithm of the INLM is shown below.

B. Joint Feature Extraction

Fusion of high-level (deep) and low-level (shallow) features is used to do joint feature extraction. Here, Deep CNN RSO is used to extract the deep features, whereas ILBP is employed to extract the low-level texture features. Both the features are cascaded to obtain joint feature extraction for performing ovarian image classification. The architecture of joint feature extraction is shown in Fig. 2.

1) Deep CNN_RSO for deep feature extraction: The high level (deep) features of the ovarian images are extracted by using the CNN (Convolutional neural network). The extracted features are then optimized using the Rat Swarm Optimization (RSO). Fig. 3 shows the DCNN's architecture. In this work, the DCNN consists of five convolutional layers: three max pooling layers and two complete reconnect layers. The activation function of each layer was a Rectified Linear Unit (ReLU). Three max pooling layers with a size of 3*3 pixels and a stride of 2 were employed to reduce the input image size of the subsequent convolutional layer. At the end of the DCNN, two fully linked layers containing a significant number of neurons were applied. The network extracts the deep features, is then optimized.

a) Rat Swarm Optimization: Rats are enormous, medium-sized rodents with long, variable-length tails. Black and brown rats are the two most common species of rats [28]. Male rats are referred to as bucks, while female rats are referred to as does. Rats are naturally smart social beings. They indulge in grooming and jumping, chasing, tumbling, and punching. Rats are territorial and inhabit colonies composed of both males and females. Rats are noted for their aggressive behaviour, which has been known to kill other creatures. This aggressive behaviour is the fundamental motivation for performing this action when pursuing and combating prey. The mathematical expression for determining the optimization value of the deep features of ovarian cancer from a CT picture using RSO is provided below.

The feature of the CT image can be found by,

$$\overrightarrow{F} = A.\overrightarrow{F}_i(x)+C(.\overrightarrow{F}_r(x)-\overrightarrow{F}_i(x)) \quad (5)$$

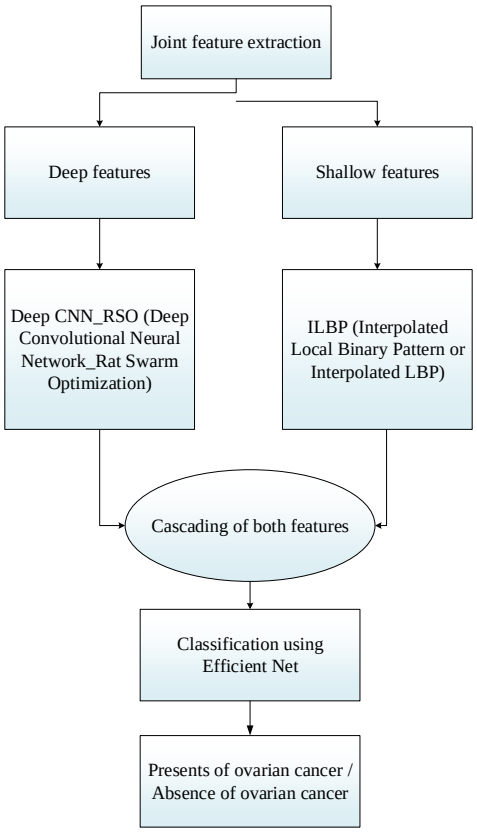

Fig. 2. Joint feature extraction.

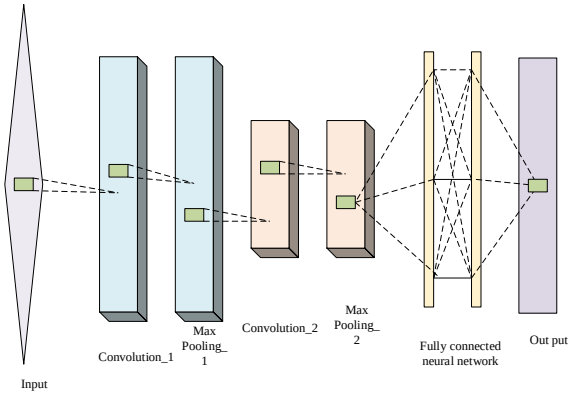

Fig. 3. DCNN's architecture.

Where $\overrightarrow{F}$ shows the deep features, $\overrightarrow{F}_i(x)$ represents the features present in the CT image, $\overrightarrow{F}_r(x)$ shows the best optimal feature, A and C shows the parameters. They can be calculated as,

$$A = R - x\times\left(\frac{R}{M_{itr}}\right) \quad (6)$$

$$x = 0,1,2,...M_{itr} \quad (7)$$

$$C = 2\cdot rand() \quad (8)$$

R is the random number between the [1, 5] and [0, 2]

The updated features can be obtained by,

$$\overrightarrow{F_{deep}} = \left| \overrightarrow{F_r}(x) - \overrightarrow{F} \right| \quad (9)$$

Here by using the Deep CNN_RSO the deep features of the CT images are extracted. Then, need to extract the shallow feature for that purpose ILBP is used.

2) Interpolated Local Binary Pattern (ILBP) for shallow feature extraction: LBP compares the grey levels of the centre pixel to the grey values of the eight neighbouring pixels in a 33 window and generates 1 or 0 to identify a pixel in the picture. It generates an eight-bit binary image as a result of the difference between grey values, with each grey value being split by its corresponding weight. Finally, these values are added together to produce a decimal value used to designate the centre pixel. Like LBP, the proposed ILBP characterizes each pixel depending on its neighbours. The only variable is that these pixels are chosen in a circular pattern and are evenly spaced in the center pixel to be labeled

Consider the position of the sampling point (X_n, Y_n) is represented as

$$x_n = x_c + R \times \cos\left(\frac{2\pi n}{N}\right),\ y_n = y_c - R \times \sin\left(\frac{2\pi n}{N}\right) \quad (10)$$

(x_c, y_c) Represents the pixel centre and $N(1 \le n \le N)$ shows the surrounding pixel number. N, R Represents the changing values of the CT image. The Generation of the circulation pattern is depicted in Fig. 4. Each phase of the circulation pattern is depicted in Fig. 4(a), (b), (c), and (d).

The grey value point $g(x, y)$ can be estimated as,

$$g(x,y) = g(0,0)(1-x)(1-y) + g(1,0)x(1-y) + g(0,1)(1-x)y + g(1,1)xy \quad (11)$$

The weight of each pixel is given as

$$P(x,y) = w_1 P_1 + w_2 P_2 + w_3 P_3 + w_4 P_4 \quad (12)$$

$$w_1 = (1-x)(1-y) \quad (13)$$

$$w_2 = x(1-y) \quad (14)$$

$$w_3 = y(1-x) \quad (15)$$

$$w_4 = xy \quad (16)$$

Interpolated LBP can be found by

$$\overrightarrow{F_{shallow}} = \sum_{n=0}^{N-1} f(I_n - I_c)2^n \quad (17)$$

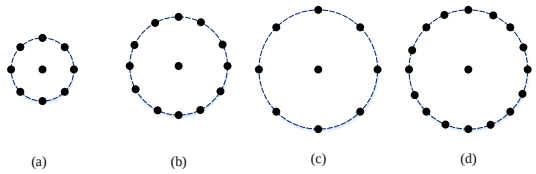

Fig. 4. Generation of circulation pattern.

$\overrightarrow{F_{shallow}}$ Represents the feature extracted by LBP, I_n *and* I_c Shows the grey value of the neighbouring pixel.

a) Joint feature: The low-level textural characteristics can characterise the edges, direction, and intensity distribution, while the high-level features retrieved from the medical CT picture can indicate the visual characteristics of the lesion's location. CNN RSO gives deep characteristics, whilst the ILBP provides shallow ones. Both CCN_RSO and ILBP output features are cascaded to form feature extraction output. The joint feature gives a better feature extraction output. The joint feature can be obtained by normalizing both the deep and shallow features. The deep feature of the picture is the network's output, and the deep feature's dimension is 1024. ILBP is utilised as the image's texture for the shallow texture feature. The ILBP element is 59 inches in length. The high and low level fusion features of an image are generated by normalising and cascading the two features.

$$\vec{F}_{shallow} = \frac{\vec{F}_{shallow} - \overrightarrow{F^{\min}}_{shallow}}{\overrightarrow{F^{\max}}_{shallow} - \overrightarrow{F^{\min}}_{shallow}} \quad (18)$$

$$\vec{F}_{deep} = \frac{\vec{F}_{deep} - \overrightarrow{F^{\min}}_{deep}}{\overrightarrow{F^{\max}}_{deep} - \overrightarrow{F^{\min}}_{deep}} \quad (19)$$

$$\overrightarrow{F_{eff}} = \left\{ \overrightarrow{F_{deep}}, \overrightarrow{F_{shallow}} \right\} \quad (20)$$

$\vec{F}_{eff}$ represents the joint feature extraction of the deep and shallow features of the ovarian cancer images, $\overrightarrow{F_{shallow}}$ Represents the feature extracted by ILBP and $\overrightarrow{F_{deep}}$ Represents the deep feature extractions.

C. Efficient Net for Classification of CT Images

The classification of the image is used to calculate the neighbourhood similarity metric. This similarity metric does not completely include the structural data of the picture whenever the noise levels are too high. The classifier follows the classification process. Here uses a classifier named Efficient Net classifier. The output of the Efficient Net is given by the global averaged features of the CT image of the ovary. On the image Net, the Efficient Net classification model delivers state-of-the-art performance. The proposed classification of the CT image follows two stages: pre-trained and training stages. The pre-trained stage frees the image weights with respect to the network. The CT image is fully retained in the second stage with an efficient net classifier.

The Efficient Net family of CNN models is based on a revolutionary scaling method. It utilizes a simple compound coefficient that is quite effective. Efficient Net scales each dimension uniformly using a predefined set of scaling factors, unlike previous approaches that scale network parameters such as breadth, depth, and resolution. In practice, increasing subjectivity improves the model's performance, but balancing all network features under available resources considerably improves overall performance. Efficient Net is considerably more compact than other variants with the same Image Net accuracy.

This research applies the Efficient Net CNN model to provide an efficient approach. This form of Efficient Net was chosen because it strikes a reasonable balance between processing resources and precision. These strategies can likewise be used to more resilient variations. Mobile inverted bottleneck convolution (MBConv) is a fundamental component of the Efficient Net model family. The Mobile Net models inspired the development of MBConv. One of the key concepts is the use of depth-wise separable convolutions, which mix depth-wise and point-wise convolution layers in succession. Fig. 5 depicts an efficient architecture for Net classifiers.

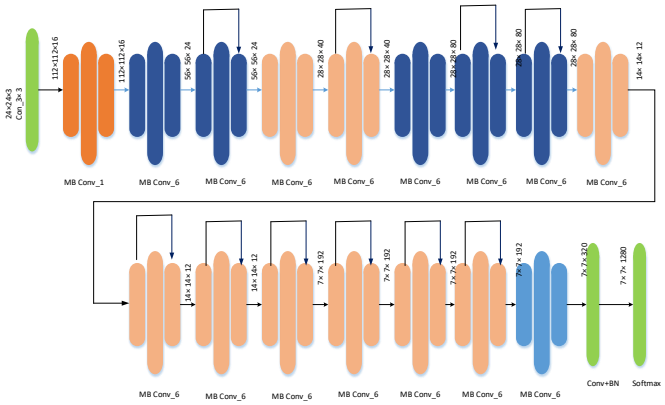

Fig. 5. Architecture of Efficient Net classifier.

The success of the previously proposed strategy for model scaling is strongly dependent on the baseline network. Searches automatically for a CNN model that maximises accuracy and efficiency (in FLOPS). The fundamental network is referred to as Efficient Net, and its essential layout is depicted in Fig. 5. The first thing to observe is that this bass line model is composed of recurring MBConv1, MBConv3, and MBConv6 blocks. These are the various sorts of MB Conv blocks. The second observation is that the number of channels per block has expanded or increased (through a bigger number of filters). The final observation relates to the inverted residual connections that exist between the thin layers of the model. Given the CT scans detection of ovarian cancer, the Efficient Net classifier output is displayed.

IV. Simulation Results

The ovarian cancer detection in the CT image using joint feature extraction and the Efficient Net model is presented using the PYTHON platform with the TCGA-OV dataset. Here the method is analyzed using sensitivity, specificity, accuracy, root mean square error (RMSE) and mean absolute percentage error (MAPE). Also, the ROC curve is obtained for the performance analysis of the system. For the classification of the features, an Efficient Net model is used. This model is analyzed by comparing the classification result using Le Net, Alex net, Google Net and VGG Net using the TCGA-OV dataset.

A. Dataset Description

1) TCGA-OV: TCIA provided a public database of abdominal CT scans used in this study: The Ovarian Cancer (TCGA-OV) dataset from the Cancer Genome Atlas. A group of researchers created the dataset. The Cancer Genome Atlas is a project examining the relationship between cancer characteristics and genetics by supplying clinical photographs. Clinical, genetic, and pathological data are stored in Genomic in TCGA-OV. TCIA stores radiological data, while the Data Commons Data Portal stores data. The TCGA-OV database contains 143 abdominal contrast-enhanced CT images and has two instances. The pelvis was outside the CT scan range, hence it was excluded from this study. The 141 remaining occurrences were included in the current investigation. The 141 samples were randomly divided into 71 training cases.

B. Performance Analysis

Here the performance of the system analyzes with respect to sensitivity, specificity, Accuracy, RMSE and MAPE. Sensitivity is the capacity to sense or respond to simulation. The equation for the sensitivity of the classifier is given as

$$\text{Sensitivity} = \frac{TP}{TP + FN} \tag{21}$$

Specificity is defined as the condition of being specific in any method. Specificity of the classifier is represented as,

$$\text{Specificity} = \frac{TN}{TN + FP} \tag{22}$$

The system's accuracy is defined as the state of being accurate in a process. The accuracy of the classifier system is given as

$$\text{Accuracy} = \frac{TP + TN}{TP + TN + FP + FN} \tag{23}$$

The RMS value is the root mean square value, and the RMSE is the process's root mean square error.

$$RMSE = 1 - \sqrt{\frac{\sum_{i=1}^{m} (T_i - P_i)^2}{N}} \tag{24}$$

The MAPE can find it as

$$MAPE = 1 - \left(\frac{\sum_{i=1}^{m} (T_i - P_i)^2}{N} \right) \times 100 \tag{25}$$

Where TP = True Positive, TN = True Negative, FP = False Positive, FN = False Negative, $i = 0,1,2...,m,\ m = \max value$.

The result obtained by each of the performance metrics is shown below. Fig. 6 shows the sensitivity of the proposed Efficient Net model with respect to other models. Here the graph shows that the sensitivity of the proposed system is 98.8% when using Le Net is 97.5%, Alex Net is 97.4&, Google Net is 97.2%, and VGG Net is 97%. Through this, the sensitivity of the proposed system is higher than that of the other classification methods.

Fig. 7 shows the specificity of the proposed method with respect to the Efficient Net. The figure shows that the specificity of the proposed method is 99.8%, the specificity of the classification method by using Le Net is 98.8%, using Alex Net is 98.6%, using Google Net is 98.4% and using VGG Net is 98.3%. Through this, the specificity of the proposed method using Efficient Net is better than that of the other classification methods.

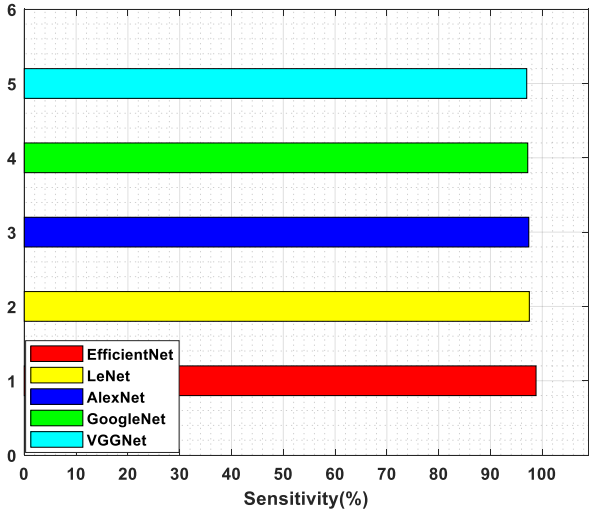

Fig. 6. Sensitivity of the proposed method.

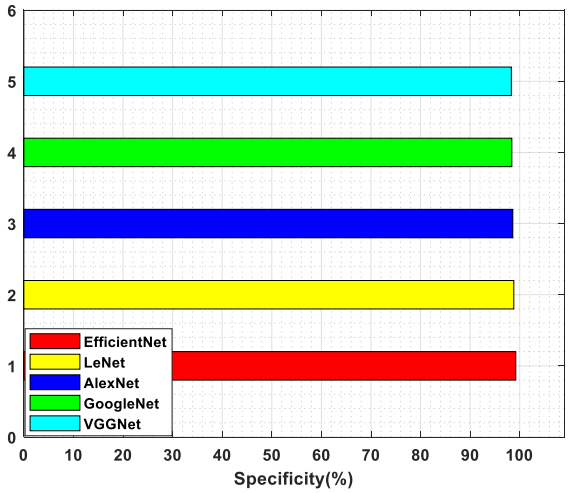

Fig. 7. Specificity of the proposed method.

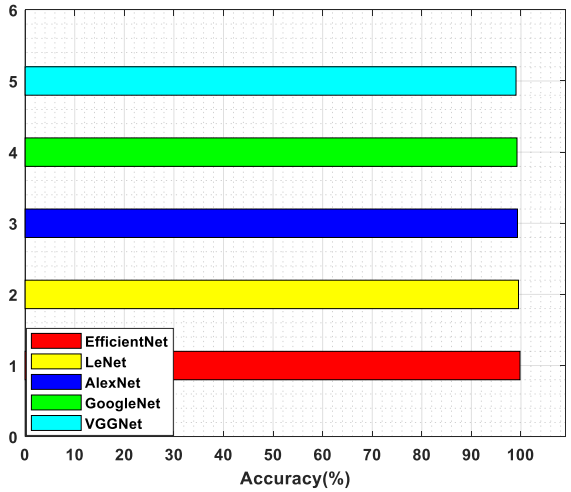

Fig. 8. Accuracy of the proposed method.

Fig. 8 shows how well the proposed method works in comparison to the Efficient Net. The graph shows that the proposed method is 99.8% accurate, the classification method is 99.5% accurate when using Le Net, 99.3% accurate when using Alex Net, 99.2% accurate when using Google Net, and 99% accurate when using VGG Net. Through this, the accuracy of the proposed method using Efficient Net is better than that of the other classification methods.

Fig. 9 shows how the proposed method compares to the Efficient Net in terms of the RMSE. The graph shows that the proposed method has an RMSE of 0.01%, the classification method using Le Net has an RMSE of 0.05%, Alex Net has an RMSE of 0.07%, Google Net has an RMSE of 0.09%, and VGG Net has an RMSE of 0.096%. Because of this, the RMSE of the proposed method using Efficient Net is better than that of the other classification methods.

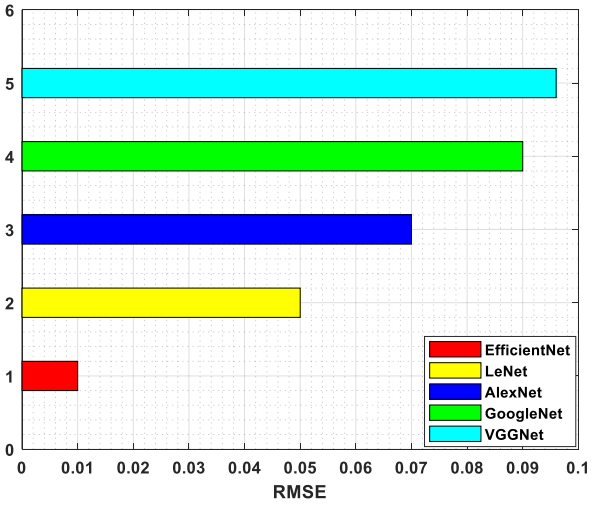

Fig. 9. RMSE of the proposed method.

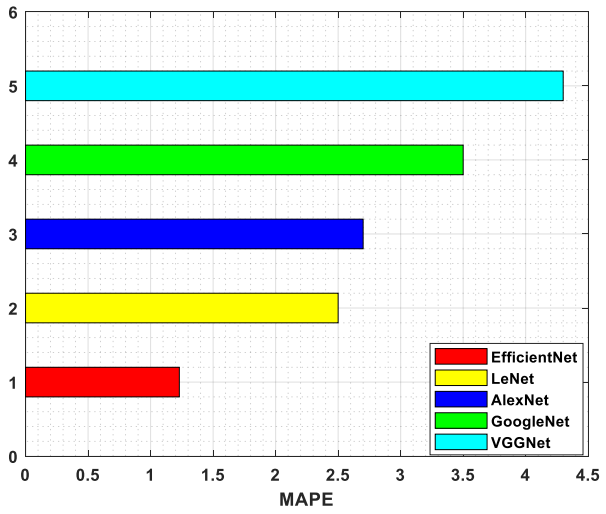

Fig. 10. MAPE of the proposed method.

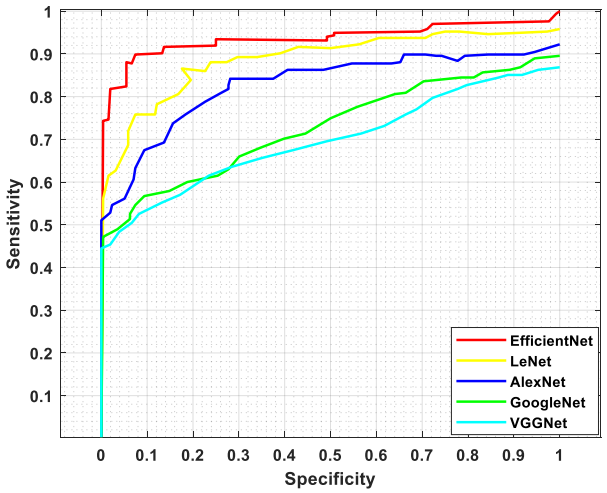

Fig. 11. ROC of the proposed method.

Fig. 10 demonstrates the MAPE of the suggested technique relative to the Efficient Net. The graph reveals that the MAPE of the suggested technique is 1.23 percent, while the MAPE of the classification method utilising Le Net is 2.5 percent, Alex Net is 2.7 percent, Google Net is 3.5 percent, and VGG Net is 4.33 percent. Consequently, the MAPE of the suggested method utilising Efficient Net is superior to that of the other categorization techniques. Fig. 11 illustrates the ROC of the proposed Efficient Net approach versus the Le Net, Alex Net, Google Net, and VGG Net. The curve demonstrates that the suggested Efficient Net model outperforms the alternatives.

V. CONCLUSION

This paper proposes ovarian cancer detection in CT images by joint feature extraction and an Efficient Net classifier. Here, the deep features are extracted using Deep CNN_RSO (Deep Convolutional Neural Network Rat Swarm Optimization) and the low-level texture features are extracted using ILBP (Interpolated Local Binary Pattern or Interpolated LBP). The cascaded feature extraction is used for the classification of the image. Also, the optimization gives better results to integrating with DCNN. The classification result shows better performance with minimum noise in the extracted images. The joint feature reduces the noise and improves the feature extraction efficiency. Finally, Efficient Net performs global average pooling and classification of ovarian cancer. By using the Efficient Net classifier, the sensitivity, specificity, accuracy, RMSE, and MAPE can be improved to 98.8%, 99.2%, 99.8%, 0.01% and 1.23%. The system's performance is compared using Le Net, Alex Net, Google Net and VGG Net using the TCGA-OV dataset. The outcome indicates that the performance of the proposed system is superior. Future work can improve the classifier's ability to classify tiny cysts in CT images.

REFERENCES

[1] J. Kemppainen, J. Hynninen, J. Virtanen, M. Seppänen, "PET/CT for evaluation of ovarian cancer," InSeminars in nuclear medicine. Vol. 49, no. 6, pp. 484-492, 2019 Nov 1. WB Saunders.

[2] B. Guo, W. Lian, S. Liu, Y. Cao, J. Liu, "Comparison of diagnostic values between CA125 combined with CA199 and ultrasound combined with CT in ovarian cancer," Oncology letters. Vol. 17, no. 6, pp. 5523-8, 2019 Jun 1.

[3] M. Shetty, "Imaging and differential diagnosis of ovarian cancer," InSeminars in Ultrasound, CT and MRI. Vol. 40, no. 4, 302-318, 2019 Aug 1. WB Saunders.

[4] M. Akazawa, K. Hashimoto, "Artificial intelligence in ovarian cancer diagnosis," Anticancer research. Vol. 40, no. 8, pp. 4795-800, 2020 Aug 1.

[5] S. Nimmagadda, M.F. Penet, "Ovarian cancer targeted theranostics," Frontiers in oncology. Vol. 9, pp. 1537, 2020 Jan 21.

[6] L. Zhang, J. Huang, L. Liu, "Improved deep learning network based in combination with cost-sensitive learning for early detection of ovarian cancer in color ultrasound detecting system," Journal of medical systems. Vol. 43, no. 8, pp. 1-9, 2019 Aug.

[7] A. Gadducci, E. Simonetti, G. Manca, F. Guidoccio, A. Fanucchi, S. Cosio, D. Volterrani, "Positron emission tomography/computed tomography in platinum-sensitive recurrent ovarian cancer: a single-center Italian study," Anticancer Research. Vol. 40, no. 4, pp. 2191-7, 2020 Apr 1.

[8] Z. Momenimovahed, A. Tiznobaik, S. Taheri, H. Salehiniya, "Ovarian cancer in the world: epidemiology and risk factors," International journal of women's health. Vol. 11, pp. 287, 2019.

[9] L. Manganaro, S. Gigli, A. Antonelli, M. Saldari, F. Tomao, C. Marchetti, E. Anastasi, A. Laghi, "Imaging strategy in recurrent ovarian cancer: a practical review," Abdominal Radiology. Vol. 44, no. 3, pp. 1091-102, 2019 Mar.

[10] P. Mohaghegh, A.G. Rockall, "Imaging strategy for early ovarian cancer: characterization of adnexal masses with conventional and advanced imaging techniques," Radiographics. Vol. 32, no. 6, pp. 1751-73, 2012 Oct.

[11] G. Di Lorenzo, G. Ricci, G.M. Severini, F. Romano, S. Biffi, "Imaging and therapy of ovarian cancer: clinical application of nanoparticles and future perspectives," Theranostics. Vol. 8, no. 16, pp. 4279, 2018.

[12] S. Nougaret, C. McCague, H. Tibermacine, H.A. Vargas, S. Rizzo, E. Sala, "Radiomics and radiogenomics in ovarian cancer: a literature review," Abdominal Radiology. Vol. 46, no. 6, pp. 2308-22, 2021 Jun.

[13] S. A. Ahmed, H. Abou-Taleb, A. Yehia, N.A. Abd El Malek, G.S. Siefeldein, D.M. Badary, M.A. Jabir, "The accuracy of multi-detector computed tomography and laparoscopy in the prediction of peritoneal carcinomatosis index score in primary ovarian cancer," Academic Radiology. Vol. 26, pp. 12, pp. 1650-8, 2019 Dec 1.

[14] S. Elsherif, S. Javadi, C. Viswanathan, S. Faria, P. Bhosale, "Low-grade epithelial ovarian cancer: what a radiologist should know," The British Journal of Radiology. Vol. 92, no. 1095, pp. 20180571, 2019 Mar.

[15] B. S. Harrington, Y. He, T. Khan, S. Puttick, P.J. Conroy, T. Kryza, T. Cuda, K.A. Sokolowski, W.C. Brian, K.K. Robbins, B.J. Arachchige,

"Anti-CDCP1 immuno-conjugates for detection and inhibition of ovarian cancer," Theranostics. Vol. 10, no. 5, pp. 2095, 2020.

[16] G. Avesani, M. Arshad, H. Lu, C. Fotopoulou, F. Cannone, R. Melotti, E. Aboagye, A. Rockall, "Radiological assessment of peritoneal cancer index on preoperative CT in ovarian cancer is related to surgical outcome and survival," La radiologia medica. Vol. 125, no. 8, pp. 770-6, 2020 Aug.

[17] S. Rizzo, M. Del Grande, L. Manganaro, A. Papadia, F. Del Grande, "Imaging before cytoreductive surgery in advanced ovarian cancer patients," International Journal of Gynecologic Cancer. Vol. 30, no. 1, 2020 Jan 1.

[18] M. Elezaby, B. Lees, K.E. Maturen, L. Barroilhet, K.B. Wisinski, S. Schrager, L.G. Wilke, E. Sadowski, "BRCA mutation carriers: breast and ovarian cancer screening guidelines and imaging considerations," Radiology. Vol. 291, no. 3, pp. 554-69, 2019 Jun.

[19] A. Meier, H. Veeraraghavan, S. Nougaret, Y. Lakhman, R. Sosa, R.A. Soslow, E.J. Sutton, H. Hricak, E. Sala, H.A. Vargas, "Association between CT-texture-derived tumor heterogeneity, outcomes, and BRCA mutation status in patients with high-grade serous ovarian cancer," Abdominal Radiology. Vol. 44, no. 6, pp. 2040-7, 2019 Jun.

[20] L. Beer, H. Sahin, N.W. Bateman, I. Blazic, H.A. Vargas, H. Veeraraghavan, J. Kirby, B. Fevrier-Sullivan, J.B. Freymann, C.C. Jaffe, J. Brenton, "Integration of proteomics with CT-based qualitative and radiomic features in high-grade serous ovarian cancer patients: an exploratory analysis," European radiology. Vol. 30, no. 8, pp. 4306-16, 2020 Aug.

[21] H. Lu, M. Arshad, A. Thornton, G. Avesani, P. Cunnea, E. Curry, F. Kanavati, J. Liang, K. Nixon, S.T. Williams, M.A. Hassan, "A mathematical-descriptor of tumor-mesoscopic-structure from computed-tomography images annotates prognostic-and molecular-phenotypes of epithelial ovarian cancer," Nature communications. Vol. 10, no. 1, pp. 1-1, 2019 Feb 15.

[22] V. Lago, P. Bello, B. Montero, L. Matute, P. Padilla-Iserte, S. Lopez, T. Marina, M. Agudelo, S. Domingo, "Sentinel lymph node technique in early-stage ovarian cancer (SENTOV): a phase II clinical trial," International Journal of Gynecologic Cancer. Vol. 30, no. 9, 2020 Sep 1.

[23] S. Wang, Z. Liu, Y. Rong, B. Zhou, Y. Bai, W. Wei, M. Wang, Y. Guo, J. Tian, "Deep learning provides a new computed tomography-based prognostic biomarker for recurrence prediction in high-grade serous ovarian cancer," Radiotherapy and Oncology. Vol. 132, pp. 171-7, 2019 Mar 1.

[24] F. Castellani, E.C. Nganga, L. Dumas, S. Banerjee, A.G. Rockall, "Imaging in the pre-operative staging of ovarian cancer," Abdominal Radiology. Vol. 44, no. 2, pp. 685-96, 2019 Feb.

[25] G. Funston, W. Hamilton, G. Abel, E.J. Crosbie, B. Rous, F.M. Walter, "The diagnostic performance of CA125 for the detection of ovarian and non-ovarian cancer in primary care: A population-based cohort study," PLoS medicine. Vol. 17, no. 10, pp. e1003295, (2020 Oct 28).

[26] S. Nougaret, M. Tardieu, H.A. Vargas, C. Reinhold, S.V. Perre, N. Bonanno, E. Sala, I. Thomassin-Naggara, "Ovarian cancer: an update on imaging in the era of radiomics," Diagnostic and interventional imaging. Vol. 100, no. 10, pp. 647-55, 2019 Oct 1.

[27] R. Forstner, "Early detection of ovarian cancer," European Radiology. Vol. 30, no. 10, pp. 5370-3, 2020 Oct.

[28] G. Dhiman, M. Garg, A. Nagar, V. Kumar, M. Dehghani, "A novel algorithm for global optimization: rat swarm optimizer," Journal of Ambient Intelligence and Humanized Computing. Vol. 12, no. 8, pp. 8457-82, 2021 Aug.